Can stationary velocity fields explain the Stokes V asymmetry observed in solar magnetic elements?

S.K. Solanki[1, 2] and K.D. Pahlke[3]

[1] Institut für Astronomie, ETH-Zentrum, CH-8092 Zürich, Switzerland
[2] Department of Mathematical Sciences, University of St. Andrews, St. Andrews KY16 9SS, Scotland
[3] Universitätssternwarte, Geismarlandstrasse 11, D-3400 Göttingen, Federal Republic of Germany

Summary. A mechanism, based on velocity gradients, for producing the observed asymmetry between the amplitudes and areas of the blue and red wings of Stokes V is discussed. It is demonstrated that line saturation is a necessary ingredient of this method, which was first proposed by Illing et al. (1975). In particular, it is shown that velocity gradients do not produce a Stokes V area asymmetry in very weak lines. Calculations using grids of parameterised models, as well as calculations which attempt to reproduce the complete Stokes V line profiles of a set of lines are presented. It is found that the observed asymmetry of lines of different strengths and excitation potentials cannot be reproduced simultaneously with a stationary velocity gradient. Also, the widths and asymmetries of strong lines cannot be reproduced simultaneously. Finally, if the asymmetries of Fe I 5250.2 Å, Fe I 6301.5 Å, and Fe I 6302.5 Å are reproduced, then their zero crossing wavelengths turn out to be too strongly redshifted as compared to the observations. Taken together these results strongly suggest that stationary flow gradients cannot account for the observed asymmetry of Stokes V.

Key words: solar magnetic fields – fluxtubes – stokes profiles – line asymmetries

1. Introduction

In the absence of mass-motions and departures from LTE, the Stokes V profile is expected to be strictly antisymmetric with respect to its zero-crossing wavelength (Auer and Heasley, 1978; Landi Degl'Innocenti and Landi Degl'Innocenti, 1981). Observations in active region plages and the quiet network show, however, that a distinct asymmetry is present with the absolute blue amplitude of Stokes V, a_b, being different from the absolute red amplitude, a_r, and the absolute area of its blue wing, A_b, being different from the absolute area of its red wing, A_r, (e.g., Stenflo et al., 1984; Stenflo and Harvey, 1985; Wiehr, 1985). For the great majority of the unblended iron lines at disk centre the blue wing dominates over the red one (Solanki and Stenflo, 1984, 1985). Near the limb the reverse is true (Stenflo et al., 1987; Pantellini et al., 1987).

The mechanisms proposed to explain the observed asymmetry (usually proposed originally to explain the broad-band circular polarization in sunspots observed by Illing et al., 1974a, b, 1975) basically fall into two categories, namely those involving mass-motions and those based on departures from LTE. Illing et al. (1975), and Grigorjev and Katz (1975) proposed a mechanism involving a combination of (stationary) velocity and magnetic field gradients to account for these asymmetries. Further calculations of varying sophistication involving velocity and magnetic field gradients were carried out by Landman and Finn (1979), Makita (1981, 1986), and Ribes et al. (1985). Auer and Heasley (1978) demonstrated that if the field is *not* parallel to the line of sight, a velocity gradient along the line of sight is alone sufficient to produce the asymmetry (cf. Landi Degl'Innocenti and Landolfi, 1983). Oscillations and/or waves with correlated velocity, temperature, and magnetic field structure have also been proposed as the source of the asymmetry (e.g. Solanki and Stenflo, 1984). Kemp et al. (1984) and Landi Degl'Innocenti (1985), on the other hand, suggest that departures from LTE combined with the anisotropy of the radiation field can give rise to differences in the populations of the Zeeman sublevels (atomic orientation), which would also result in a Stokes V asymmetry.

So far no convincing arguments which rule out any of these mechanisms have been published, although Solanki (1985, 1986) has presented evidence in favour of a connection between mass-motions and asymmetry. In this paper we present the results of a quantitative test of the hypothesis of Illing et al. (1975) and Grigorjev and Katz (1975). We compare observed Stokes V profiles (disk centre recordings; see Stenflo et al., 1984 and Scholiers and Wiehr, 1985 for a description of the data) with the results of LTE calculations, carried out with two slightly different approaches and using two different radiative transfer codes (the code described by Wittmann, 1974, in Sect. 3.2; and a modified version of the code of Beckers, 1969, in Sects. 3.1 and 4). Both sets of calculations have in common that they are based on simple fluxtube models containing a steady flow with a vertical gradient. All calculations are restricted to single lines of sight along the axes of vertical fluxtubes at disk centre ($\mu = 1$).

Some general considerations and analytical calculations are presented in Sect. 2. In Sect. 3 we present results of line profile calculations in two grids of models which cover a wide range of parameters. This systematic survey allows us to form an idea of how the Stokes V asymmetry reacts to various atmospheric

parameters, and helps to show which values of the atmospheric parameters reproduce the observed asymmetry. In Sect. 4 we then attempt to reproduce the observed Stokes V line profiles of four lines simultaneously, and finally in Sect. 5 we summarize the conclusions drawn from this work. A preliminary report of a part of this work has been published previously (Pahlke and Solanki, 1986).

2. Stokes V asymmetry produced by velocity gradients: general considerations

There are two variants of the basic mechanism for producing the asymmetry with a velocity gradient. The first requires both magnetic field strength B and velocity v to vary along the line of sight (i.e. it requires both the wavelength difference between the σ components and their central position to change with optical depth). This is the mechanism proposed by Illing et al. (1975). The second mechanism requires just a velocity gradient along the line of sight, but it works only when the line of sight is not parallel to B. Then the relative strengths of the absorption coefficients of the σ and π components change along the line of sight, i.e. the shapes of the absorption coefficients for left and right circularly polarized light change with optical depth, as do their wavelengths (but not the wavelength difference between them). This mechanism was first proposed by Auer and Heasley (1978). It is based on the coupling between the σ and π components via the transfer equation when $\gamma \neq 0$ (γ is the angle between B and the line of sight) and additionaly requires different heights of formation for the σ and π components. Since the field of magnetic elements is not expected to be either vertically or horizontally homogeneous (due to the vertical drop in gas pressure and due to the finite width of magnetic elements), we would, for the genral case ($\gamma \neq 0$ and $dB/dr \neq 0$), expect the asymmetry to be caused by a combination of the two effects which are both automatically taken into account by radiative transfer codes. An advantage of the Auer and Heasley mechanism is that it allows an analytical solution under certain assumptions. We shall, therefore, later use it to show that the area asymmetry disappears for very weak lines. On the other hand, for many lines the asymmetry is not seen to decrease near disk centre as would be expected if the Auer and Heasley mechanism were the dominant one. Therefore, we shall first consider the mechanism of Illing et al. in greater detail.

Figure 1 illustrates schematically how the Stockes V asymmetry can be produced in a very simple model consisting of two plane parallel slabs lying on top of each other. We assume that $\mu = 1$ and that the magnetic field is vertical. Then the radiative trnasfer equations for circular and linear polarization decouple and we can consider right and left circularly polarized light independently (Stepanov, 1958a, b; Stenflo, 1971). In the bottom frame $\eta \pm$, the ratio of the line to continuum absorption coeffic- ients for right and left circularly polarized light, are shown at a depth in the atmosphere where B is large and $v \approx 0$. In the second lowest frame $\eta \pm$ are shown higher up in the atmosphere where B is small and v is large and positive. We use the usual sign convention: $v(\tau) > 0$ for downflows. The third frame from the bottom shows the emergent profiles $I_{\pm}(\tau = 0)$ (i.e. the intensity profiles of right and left circularly polarized light coming from inside the magnetic element) and finally the top frame shows the corresponding Stokes V profile, $V = I_+ - I_-$. The difference between the *areas* of I_+ and I_-, and therefore also the asymmetry in Stokes V is produced by a combination of saturation effects
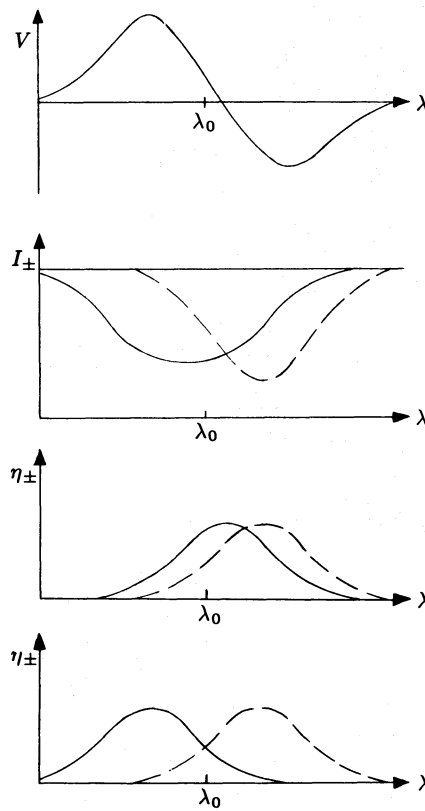

Fig. 1. Bottom frame: $\eta_{\pm}$ (absorption coefficients for right and left circularly polarized light) deep in the atmosphere. Second lowest frame: $\eta_{\pm}$ higher in the atmosphere. Third lowest frame: $I_{\pm}$, the emergent intensity profiles for the two polarizations. Topmost frame: $V = I_+ - I_-$

and gradients in $v(\tau)$ and $B(\tau)$. It is important to note that without saturation we obtain no asymmetry between the areas of the red and blue wings of Stokes V. In reality, due to limited spatial resolution, light from the non-magnetic surroundings is mixed with $I_{\pm}$, but when creating Stokes V this light does not contribute (to first order), so that we need not include it in Fig. 1. λ_0 is the laboratory wavelength of the line, λ_V the zero-crossing wave- length of Stokes V. Note the redshift, $\lambda_V - \lambda_0$ of Stokes V in Fig. 1.

As is suggested by the figure, it is the *gradients* of B and v which are important for the production of the asymmetry if the field is parallel to the line of sight. In particular, the absolute value of v has no effect on the asymmetry, so that we can write

$$v(\tau) = v_0 + v_1(\tau) = v(\tau_0) + (v(\tau) - v(\tau_0)), \tag{1}$$

with τ_0 chosen such that the contribution function of the line is approximately zero there. $v_0 = v(\tau_0)$ is an arbitrary constant velocity as far as the asymmetry is concerned. Note, however, that this is not true for B_o [if we write in analogy to Eq. (1): $B(\tau) = B_0 + B_1(\tau)$], since the magnetic field affects the line profile in a completely different manner.

Figure 1 also illustrates another simple point. Near disk centre for all but the very strongest lines in the visible spectral range the observed asymmetry is almost always such that the blue wing of Stokes V dominates over its red wing, i.e. $\delta a > 0$ and $\delta A > 0$. $\delta a = (a_b - a_r)/(a_b + a_r)$ is the relative amplitude asymm- try, where a_b and a_r are the absolute amplitudes of the blue and red Stokes V wings, respectively. δA is the similarly defined

relative area asymmetry. In order to reproduce the observed sign of δA

$$\frac{d|B(\tau)|}{d\tau}\frac{dv(\tau)}{d\tau} < 0 \tag{2}$$

must be true in the region of the formation of these lines at disk centre. The fact that only the absolute value of $B(\tau)$ is important, while the sign of $v(\tau)$ also plays a role is again due to the different ways in which v and B affect the line profile. The simple heuristic model discussed above can furthermore be used to show that for B perpendicular to the line of sight Stokes Q also shows an asymmetry between its blue and red σ components in the presence of velocity and magnetic field gradients along the line of sight. If Eq. (2) is assumed to be valid, then the blue σ component is stronger than the red one (τ is measured along the line of sight). Radiative transfer calculations confirm this.

Equation (2) has some straightforward, but interesting consequences. If $d|B(\tau)|/d\tau > 0$ (i.e. magnetic field strength *decreasing* with geometrical *height*), then for a downflow the velocity must decrease with τ, while for an upflow it must increase with τ. In the former case we expect the resulting Stokes V profile to be redshifted, while in the latter case we expect a blueshift. Of course, it is always possible to choose v_0 in Eq. (1) such that the emergent line profile shows no shift relative to its rest wavelength. However, if we want to interpret $v(\tau)$ as a stationary flow inside fluxtubes then we must require that the sign of v does not change at any height in the fluxtube photosphere. Since the possible $v_1(\tau)$ values are constrained by the observed asymmetry, this additional condition greatly limits the choice of v_0. Thus it may no longer be possible to reproduce both the observed profile shape and zero-crossing shift with a stationary flow. In the following sections we present the results of some model calculations which test this point. In order not to be unduly restrictive we shall also accept $v(\tau)$ functions which retain their sign only over the height range over which the calculated lines show any sensitivity to the velocity.

The Auer and Heasley (1978) variant of the basic mechanism can also be discussed in a simple heuristic manner similar to the discussion given in the previous few paragraphs. It is then evident that the asymmetry produced by this variant is equally dependent on line saturation.

The crude model presented above suggests that very weak lines, with no saturation, should have Stokes V profiles with disappearing area asymmetry. This can be proved analytically for the model of Auer and Heasley (1978), which assumes a static Milne-Eddington atmosphere with constant field strength B overlain by a thin moving layer with the same field strength and the velocity v.

In a Milne-Eddington atmosphere [Planck function linear in τ, $B_\nu = B_{\nu_0}(1 + \beta_0\tau)$] we obtain for the (unnormalised) V profile emerging from the underlying static layer (if we neglect magnetooptical effects, e.g., Unno, 1956)

$$V = -\frac{B_{\nu_0}\beta_0\mu}{D}\eta_V(0), \tag{3}$$

where $\mu = \cos\theta$, where θ is the heliocentric angle,

$$D = (1 + \eta_I(0))^2 - \eta_Q^2(0) - \eta_U^2(0) - \eta_V^2(0), \tag{4}$$

and $\eta_I(0)$, $\eta_Q(0)$, $\eta_U(0)$, $\eta_V(0)$ are the ratios of line to continuum absorption coefficients for Stokes I, Q, U, V respectively in a static

atmosphere. Expressions for $\eta_I, \eta_Q, \eta_U, \eta_V$ have been given by, e.g., Wittmann (1974). The linearised change in the V profile caused by the thin moving layer is

$$\Delta V = \frac{\Delta\tau B_{\nu_0}\beta_0}{D}\left(\eta_V(v)\left(1 - \frac{D}{\beta_0\mu}\right)\right.$$
$$\left. + \eta_V(v)\eta_I(0) - \eta_V(0) - \eta_V(0)\eta_I(v)\right), \tag{5}$$

where $\eta_V(v)$ and $\eta_I(v)$ represent the line absorption coefficients in the moving layer of velocity v. Note that $\eta_I(v)$ is symmetric around $x = (\lambda - \lambda_0)c/\lambda_0 = v$, while $\eta_V(v)$ is antisymmetric with respect to $x = v$. The final emergent profiles is then

$$V_{\text{tot}} = V + \Delta V = \frac{\Delta\tau B_{\nu_0}}{D}\beta_0\left(\eta_V(v)\left(1 - \frac{D}{\beta_0\mu}\right) + \eta_V(v)\eta_I(0)\right.$$
$$\left. - \eta_V(0)\eta_I(v) - \eta_V(0)\left(1 + \frac{\mu}{\Delta\tau}\right)\right). \tag{6}$$

For a very weak line with $\eta_I \ll 1$ and $\eta_V \ll 1$ we have $D \approx 1$, $\eta_V(v)\eta_I(0) \ll \eta_V(v)$, and $\eta_V(0)\eta_I(v) \ll \eta_V(0)$, so that Eq. (6) reduces to

$$V_{\text{tot}} = \Delta\tau B_{\nu_0}\beta_0\left(\eta_V(v)\left(1 - \frac{1}{\beta_0\mu}\right) - \eta_V(0)\left(1 + \frac{\mu}{\Delta\tau}\right)\right). \tag{7}$$

The emergent Stokes V profile is therefore a sum of two profiles which are antisymmetric about $x = 0$ and $x = v$, respectively. Although the profile shape need not be antisymmetric, it will not exhibit any *area* asymmetry. Therefore very weak lines will have $\delta A \approx 0$ for any combination of "stationary" flow gradients. Such combinations include a distribution of up-, and downflows in an ensemble of fluxtubes, or oscillations or waves observed with low temporal resolution. The observation of very weak lines therefore provides a possible method of deciding whether velocity gradients along the line of sight are in one form or another responsible for the area asymmetry of Stokes V. If the weakest Stokes V profiles exhibit an asymmetry between the areas of their red and blue wings then we can rule out velocity gradients as a source of this asymmetry.

3. Calculations using grids of parameterised models

3.1. Models with a linear velocity structure

In this section we present numerical calculations of Stokes V profiles which serve to investigate the diagnostic contents of the Stokes V asymmetry and to test how the simple picture presented in Sect. 2 compares with the results of numerical radiative transfer calculations.

Restricting $B(\tau)$ and $v(\tau)$ to functions linear in τ, we have tested how the asymmetry of a line is influenced by its strength, excitation potential, and Zeeman splitting. We have calculated the profiles of the Fe I 5250.2 Å line as well as of hypothetical iron lines which differ from Fe I 5250.2 Å in only one parameter at a time, e.g. in excitation potential χ_e, in Zeeman splitting, or in line strength. Since lines of different strengths and excitation potentials are formed at different heights in the atmosphere, the choice of constant B and v gradients ensures that all lines are treated approximately equally. This restrictive choice of $v(\tau)$ is limited to this section only. In Sect. 3.2 we use an exponential $v(\tau)$, while in Sect. 4 we allow for arbitrary $v(\tau)$ profiles. In the following we list some of the results.

—We find that δA always has the signs predicted by Eq. (2) for both up- and downflows.

—Whereas δA is always positive for $d|B|/d\tau > 0$ and $dv/d\tau < 0$, δa can be either positive or negative. Its value depends on the exact velocity gradient and on the spectral line. Thus, for diagnostic purposes δA is better for determining the outline of the velocity structure, while the amplitude asymmetry is more sensitive to the details.

—δA is only weakly dependent on the Landé factor for the cases we have tested. This also suggests that the absolute value of B is not of dominating importance. It is possible that the last result is an artifact of the limited number of model calculations testing this.

—δa is somewhat dependent on Landé factor. δa often tends to become more negative with increasing Zeeman splitting, although this dependence is itself a function of velocity gradient.

—The area asymmetry increases strongly with the amount of saturation in the line. For lines of equal excitation potential, this means that δA increases rapidly with increasing line strength. This result is in agreement with the predictions of the simple model described in Sect. 2.

—δa also shows an increasing tendency to become positive as the amount of saturation increases, but this trend is not so marked.

—For a given line and an otherwise unchanged atmosphere, an increase in temperature leads to a decrease in the calculated asymmetry of that line. This effect is small for Fe II lines and markedly larger for Fe I. It increases dramatically with *decreasing* excitation potential (for lines of equal strength in the original atmosphere), and is mainly due to the temperature induced weakening and the associated decrease in saturation of the lines.

—The line shapes calculated with linear $v(\tau)$ are not in the least similar to the observations, even if we use a $B(\tau)$ calculated via the thin tube approximation. For example, synthetic Fe I 5250.2 Å profiles have $\delta A > 0$ but $\delta a < 0$, while the observations show that both δA and δa are positive.

3.2. Models with an exponential velocity structure

We present radiative transfer calculations of Fe I 6301.5 Å and Fe I 6302.5 Å, which have been carried out in a grid of parameterised models and have been compared to the values of δa, δA, and v_{VI} (the Stokes V zero-crossing wavelength shift with respect to Stokes I, in velocity units) observed for these lines by Scholiers and Wiehr (1985 and private communication) and Stenflo et al. (1984). The atomic parameters of these two lines are summarized in Table 1. Each of the models considered in this section has a

velocity and magnetic field structure of the following simple forms

$$v(\tau) = v_0 \exp(\omega \log \tau) - v_0, \tag{8}$$

$$B(\tau) = B_0 \exp(\beta \log \tau), \tag{9}$$

where ω and β are dimensionless quantities. Together with v_0 and B_0 there are thus four free parameters per model. The second term on the right hand side of Eq. (8) has been introduced to minimise the resulting redshift [this term makes $v(\tau = 1) = 0$], in order to reproduce the observations as well as possible. We restrict ourselves to downflows in this and the next section, i.e. $v_0 > 0$ and $\omega < 0$ (velocity decreases with increasing optical depth).

Calculations have been carried out with these $v(\tau)$ and $B(\tau)$ functions for an extensive set of parameters and a number of model atmospheres. First a smaller grid was calculated for Fe I 6302.5 Å alone, but for a variety of $T(\tau)$ structures. Among others we used the facular models of Chapman (1979), the filigree model of Stellmacher and Wiehr (1979) and the fluxtube models of Solanki (1986). Some of the results of these calculations and how they compare to the observations have been presented by Pahlke and Solanki (1986) and we shall not discuss these calculations in detail here. In contrast to the models with a linear $v(\tau)$ the exponential models can reproduce the approximate observed δA and δa simultaneously, although there are some differences between the results of the various temperature models. We found that the plage model of Solanki (1986) reproduces the observed amplitude and area asymmetries best, followed by the model of Stellmacher and Wiehr (1979). This may be due to the particular form of the chosen velocity and magnetic field functions. However, *none of the models was able to reproduce the asymmetries and the zero-crossing wavelengths simultaneously.*

After these initial calculations we have concentrated on just two temperature structures, the model of Stellmacher and Wiehr (1979) and the plage model of Solanki (1986), while retaining Eqs. (8) and (9) for $v(\tau)$ and $B(\tau)$. The profiles of both Fe I 6301.5 Å and 6302.5 Å have been calculated using these models for an extensive grid of the four free parameters. As an example the results of one sub-grid of calculations using the plage model of Solanki (1986) are illustrated in Figs. 2a–f. In the calculations illustrated in this figure (δa in Figs. 2a and b. δA in Figs. 2c and d, and v_{VI} in Figs. 2e and f) we have kept $B = 1500$ G and $\beta = 0.75$ fixed, while varying ω and v_0. The curves marked 1, ..., 6 correspond to $v_0 = 0.25, 0.50, 0.75, 1.00, 1.25$ and 1.5 km s^{-1}, respectively. First we list some of the general results before turning to the comparison with observations.

—δA increases with the parameters ω and v_0 for small values of ω, respectively v_0. However, for large ω and v_0 it can decrease again.

Table 1. List of calculated lines

Ion	λ(Å)	Multiplet	Transition	χ_e(eV)	g_{eff}
Fe I	5083.3450	16	$a^5F_3 - z^5F_3^0$	0.96	1.250
Fe I	5127.6836	1	$a^5D_3 - z^7D_2^0$	0.05	1.000
Fe II	5197.5742	49	$a^4G_{2\frac{1}{2}} - z^4F_{1\frac{1}{2}}^0$	3.23	0.700
Fe I	5250.2171	1	$a^5D_0 - z^7D_1^0$	0.12	3.000
Fe I	6301.5091	816	$z^5P_2^0 - e^5D_2$	3.65	1.667
Fe I	6302.5017	816	$z^5P_1^0 - e^5D_0$	3.69	2.500

In other words, for small velocity gradients δA increases with the velocity gradient, while for large gradients this is no longer necessarily the case.

—δA is a monotonic increasing function of β, i.e. of the gradient of B (B_0 is kept fixed).

—δa shows a less clear dependence on these parameters. The general tendency is for it to increase with v_0, ω and β, although exceptions to this rule may be seen in Figs. 2a and b.

—For the tested cases Eq. (2) is satisfied.

—δa can be both positive or negative. However, for exponential velocity structures it is at most slightly negative and that only for small ω.

—v_{VI} is always positive, i.e. the lines are redshifted (recall that we consider only the case $v_0 > 0$ and $\omega > 0$).

—v_{VI} always increases strongly with ω and v_0, as expected. However, it decreases slightly with increasing β as the lines are formed deeper where the field is stronger (B. Larsson, private communication).

The above results are qualitatively the same for both lines. They once more illustrate the totally different manner in which the magnetic and velocity fields affect the line profile. Other results are different for the two lines:

—Fe I 6302.5 Å, being somewhat weaker, always shows a smaller calculated asymmetry than Fe I 6301.5 Å, in agreement with the discussion in Sect. 2.

—Fe I 6302.5 Å, being formed deeper in the atmosphere, where v is smaller, generally has a somewhat lower redshift.

—For Fe I 6301.5 Å δa is a monotonic increasing function of β for all β values, while for Fe I 6302.5 Å this is the case only for large β.

The data which these calculations are compared with have mostly been obtained by Scholiers and Wiehr (1985 and private communication). The area and amplitude asymmetry of Fe I 6301.5 Å and 6302.5 Å was determined for 16 regions, while the zero crossing wavelength is available for 11 regions, all of which were located near disk centre. In addition we have also compared the profiles of these lines with those obtained with the Fourier Transform Spectrometer (FTS) attached to the McMath telescope at Kitt Peak (Stenflo et al., 1984). The measured asymmetries (δa, δA) and the shifts of the zero-crossing wavelengths with respect to the Stokes I wavelengths, v_{VI}, are summarized in Table 2. The notation of regions corresponds to Scholiers and Wiehr (1985), except for the two FTS spectra which are named following Solanki (1987). In the second last row of Table 2 the parameters averaged over all the observed values are listed, while the last column lists the σ values of these averages. For all regions the blue wing has a larger area than the red wing and in all except one region this is also the case for the amplitude. The average v_{VI} values are practically zero, but there is considerable scatter in all three quantities. Note that the v_{VI} values have been listed without taking into account the granular blueshift of Stokes I. The scatter is only partly due to noise, since δa, δA and v_{VI} of Fe I 6301.5 Å are correlated with the corresponding parameters of Fe I 6302.5 Å. As far as the v_{VI} are concerned, it cannot be decided whether this scatter comes from Stokes V, e.g., due to different velocities in different magnetic elements or from a variation of Stokes I from region to region (e.g., due to the five minute oscillations).

A quantitative comparison of the calculated with the observed profiles reveals major differences between the two. Firstly, none of the profiles with negative v_{VI} can be reproduced, since for all the model calculations $v_{VI} > 0$. For both Fe I 6301.5 Å and 6302.5 Å it is possible to approximately reproduce the zero-crossing shifts and δa or δA of only three of the observed profiles. The lines in these three regions exhibit small asymmetries and at the same time large redshifts. δa and δA together can be roughly reproduced for a larger number of observed regions, but the calculated, v_{VI} is then much too large. The observations also show both lines to have approximately the same asymmetry (within the errors), which contradicts the model calculations. In Figs. 2a–f, in addition to the model calculations, we have also plotted the data observed in four regions from Table 2 for which δa and δA are simultaneously reproduced (within the errors) by the particular set of parameters illustrated in the figure (dashed horizontal lines). The average observed values of the parameters have also been plotted (solid horizontal lines). Each data value is represented by a horizontal dashed line. Note that for region D the v_{VI} plotted in Figs. 2e and f are absolute values, since the observed values are negative (blueshifts) and as a result would lie outside the frames.

4. Models reproducing the complete line profile

In this section we summarize some of the results of calculations aimed at reproducing the complete observed Stokes V line profiles. In contrast to the previous section, the model atmosphere is specified point by point at all depths.

We have tried to simultaneously reproduce the V asymmetry of four lines selected from Table 1, namely Fe I 5250.2 Å, 5127.7 Å, 5083.3 Å, and Fe II 5197.6 Å. The first three are low excitation potential (χ_e) Fe I lines with strongly different line strengths, while 5197.6 Å is an Fe II line slightly stronger than 5250.2 Å in the quiet sun. These four lines form a subset of the ten lines selected by Solanki (1986) for empirical fluxtube modelling. The lines at 6302.5 Å and 6301.5 Å are not discussed in this section, since their profiles were not observed simultaneously with those of the other four lines. We have used a number of temperature models: the plage and network models derived by Solanki (1986), a model with $T(\tau)$ similar to that of Chapman (1979), and models with $T = T_{HSRA} + \Delta T$, where $\Delta T = 400$ K and 800 K, and $\Delta T \neq \Delta T(\tau)$. Initially we chose the magnetic field as calculated with the thin tube approximation, with $B(\tau = 1) = 2000$ G, as suggested by the results of Solanki et al. (1987). Since the internal gas pressure was obtained by requiring hydrostatic equilibrium, this means that the magnetic field was calculated consistently with the temperature structure. Later $B(\tau)$ was allowed to be specified freely in an attempt to reproduce the spectral lines better. No constraints have been set on the $v(\tau)$ structure throughout the calculations discussed in this section, except for the constraints set on the constant component v_0 in Sect. 2. The calculations procedure was as follows: We first determined $v(\tau)$ [and later also $B(\tau)$] by trying to reproduce one particular line profile, usually Fe I 5250.2 Å, and then calculated the other profiles with the same atmosphere and velocity structure.

In Fig. 3 we have plotted examples of the observed and calculated profiles of the four selected lines. The observations were obtained in an active region plage (they have been described by Stenflo et al., 1984 and Solanki, 1987). Their S/N is very high, so that all except the smallest spectral features can be considered to be real (noise is of the order of $1–2 \, 10^{-4}$). The calculations were carried out using the plage temperature model. Since we are at the moment only interested in the V profile *shapes*, the synthetic
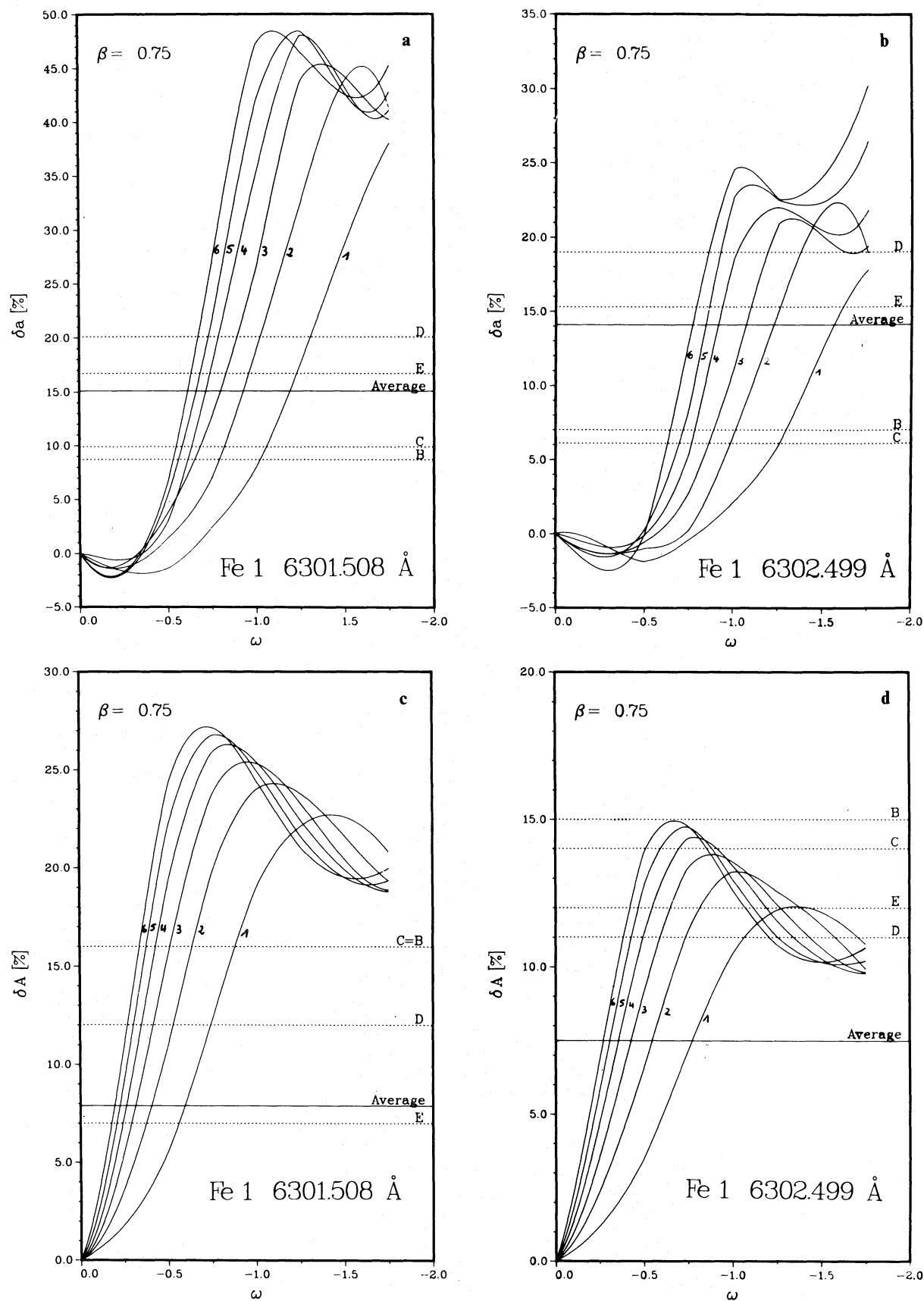
Fig. 2a–f. Stokes V relative amplitude asymmetry δa (**a**, **b**), relative area asymmetry δA (**c**, **d**) and red-shift of the zero-crossing wavelength relative to Stokes I in velocity units, v_{VI} (**e**, **f**) vs. the velocity gradient ω for Fe I 6301.5 Å (**a, c, e**) and Fe I 6302.5 Å (**b, d, f**). The curves marked 1 . . . 6 correspond to $v_0 = 0.25, 0.5, 0.75, 1.0, 1.25, 1.5$ km s^{-1}, respectively. The horizontal dashed lines represent examples of the observed values in the regions denoted B, C, D and E by Scholiers and Wiehr (1985), while the horizontal solid lines represent average values of the observed parameters. Note that in **e** and **f** only the absolute values of the negative v_{VI} of region D have been plotted
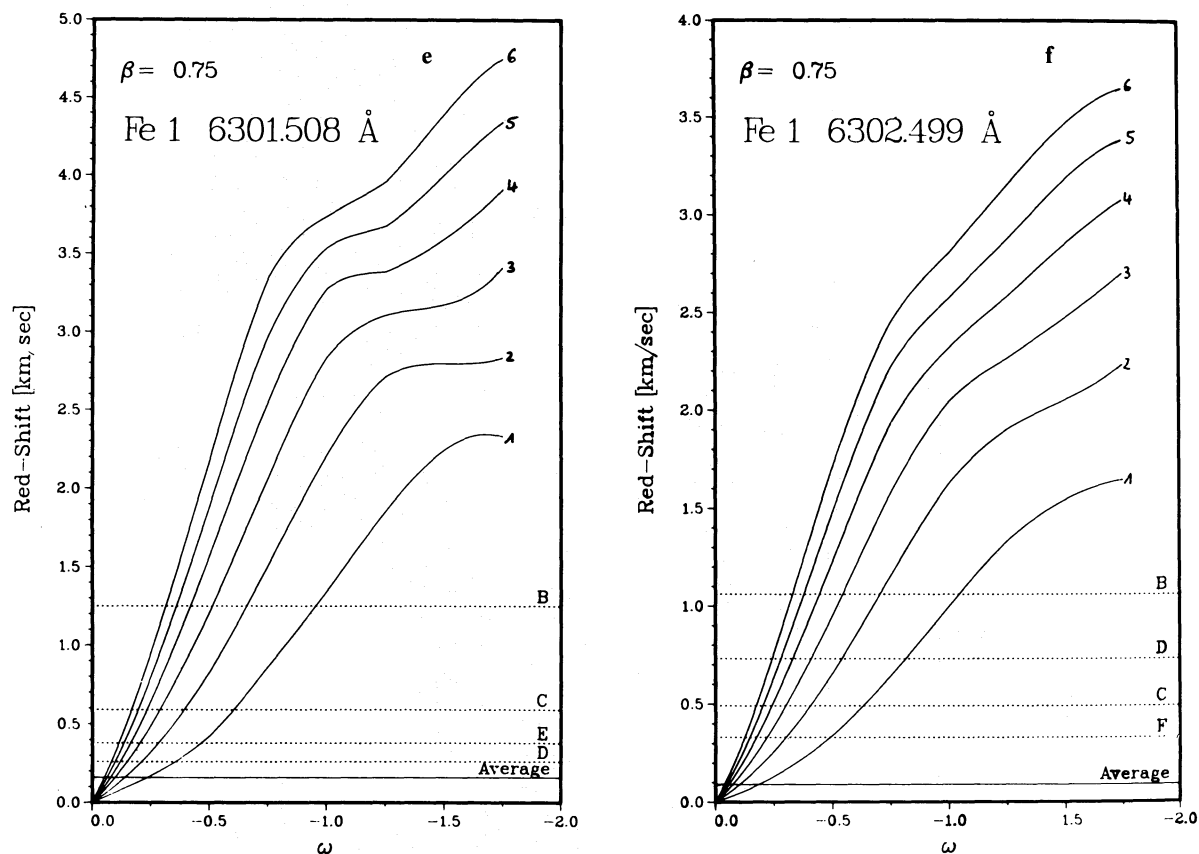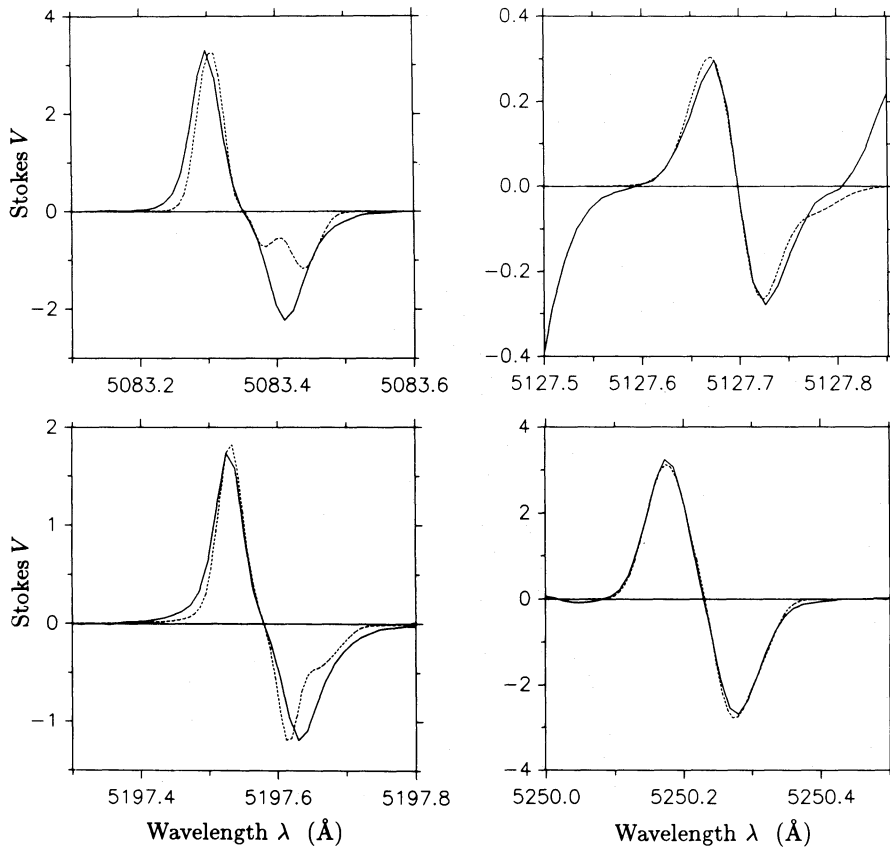
Fig. 2 (continued)

Table 2. Observed Stokes V parameters

Region	Fe I 6301.5 Å			Fe I 6302.5 Å		
	δa (%)	δA (%)	v_{VI} (km s^{-1})	δa (%)	δA (%)	v_{VI} (km s^{-1})
FTS3	18.9	2	0.27	17.8	6	0.40
FTS5	12.6	4	0.00	9.3	5	0.21
A	6.1	0	0.75	−5.3	0	0.88
B	8.7	16	1.25	7.0	15	1.06
C	9.9	16	0.59	6.1	14	0.49
D	20.1	12	−0.26	19.0	11	−0.73
E	16.7	7	0.38	15.3	12	0.33
F	16.3	7	−0.14	16.7	13	0.00
G	12.7	0	−0.63	14.2	0	−1.13
H	8.7	0	0.31	15.3	0	0.53
I	19.0	10	−0.25	20.0	6	−0.31
J	33.3	25	−0.25	29.3	16	−1.00
K	17.7	10	0.00	20.6	9	−0.38
I	14.5	3	—	7.8	0	—
II	20.0	9	—	19.0	14	—
III	12.3	5	—	12.7	4	—
IV	11.9	9	—	15.3	4	—
V	13.8	8	—	14.2	8	—
Average	15.1	7.9	0.16	14.1	7.5	0.09
σ	6.1	6.3	0.49	7.2	5.5	0.66

Fig. 3. Profiles of Fe I 5083.3 Å, Fe I 5127.7 Å, Fe II 5197.7 Å, and Fe I 5250.2 Å, as observed in an active plage (solid curves) and calculated (dashed curves) using a stationary downflow, which is chosen such that the Fe I 5250.2 Å profile is reproduced. The calculated profiles have been shifted and normalized to the amplitudes of the observations

profiles have been shifted and multiplied by factors to make them match the data better.

Although 5127.7 Å can be reproduced reasonably well simultaneously with 5250.2 Å, the synthetic 5083.3 Å profile does not fit the data at all. While the calculated values of the relative area asymmetry, $\delta A(5127) = 0.7\%$, $\delta A(5250) = 5.1\%$, and $\delta A(5083) = 28.1\%$, increase steadily with line strength, in accordance with the results of the test calculations of Sect. 3.1, this is not true for the observed values, with $\delta A(5127) = -1.8\%$, $\delta A(5250) = 5.3\%$, and $\delta A(5083) = 5.2\%$. Thus the observed 5250.2 Å and 5083.3 Å profiles have approximately equal relative asymmetry which leads to a mis-match between the data and the calculations. The relative behaviour of these lines is similar for the other models as well, none of which reproduces the data any better.

We have also tried improving the fit to 5083.3 Å alone, but the fit to 5250.2 Å then begins to deteriorate. Only 5127.7 Å remains almost unchanged, due to the relative insensitivity of its profile shape to velocity gradients. Actually, 5083.3 Å is a problem in itself, since its complete V profile is very difficult to reproduce. In order to check whether this problem is due to a hidden blend, or some other peculiarity of this particular line, we have also briefly used the Fe I 5127.3 Å line, which has an excitation potential and line strength similar to 5083.3 Å. However, 5127.3 Å also exhibits the same behaviour.

The difficulty stems from the fact that the observed asymmetry of the strong low excitation lines requires the presence of relatively small velocity gradients, while, at the same time, these lines are also considerably velocity broadened (Solanki, 1986). In fact, such lines have nearly the largest velocity broadening in

magnetic elements of all the unblended Fe I lines. Therefore, if a stationary flow with a small gradient is chosen as the only velocity in the fluxtube, then the line width cannot be reproduced. If, on the other hand, we try to reproduce the large width with a velocity gradient alone, an immense value is required and the asymmetry becomes much too large.

A possible way out of this dilemma is to use a combination of stationary velocity with a small vertical gradient and a turbulence velocity, composed for example of a micro- and a macroturbulence. The former produces the asymmetry, while the latter gives the line the required width. Although the resulting profile does not yet have the right shape, it is considerably closer to the observed profile than if any one of the mechanisms is used alone. Nonetheless, a stationary flow inside the magnetic element cannot by itself account for the profile of Fe I 5083.3 Å.

When using the velocity derived by fitting Fe I 5250.2 Å to calculate Fe II 5197.6 Å we find that the V profile of this line also has a too large asymmetry compared to the observed profile ($\delta A_{calc} = 11.4\%$ for the plage model, while $\delta A_{obs} = 4.4\%$), although the amplitude asymmetry is similar to the observed one (Fig. 3). The factor of two larger asymmetry of the calculated Fe II 5197.6 line profile compared to that of Fe I 5250.2 Å is mainly due to the fact that the former is weakened considerably less by the higher temperature of the fluxtube model.

We have also observed that all the good fits to the shape of Fe I 5250.2 Å, involving only a stationary downflow, have a zero-crossing wavelength shifted towards the red by a value greater than approximately 0.9 km s^{-1}. This shift is the result of the velocity having the same sign over the whole photosphere. Note

that we reduce the shift to a minimum by setting $v = 0$ just below the height at which the line starts to become sensitive to the velocity gradient. This choice is quite conservative, since, due to mass conservation, the velocity cannot disappear completely. It implies that 0.9 km s^{-1} is a true lower limit to the zero-crossing shift of the synthetic profiles for the models considered. Therefore, the observational constraint that the temporally and spatially averaged Stokes V zero-crossing shift is less than 0.25 km s^{-1} (Stenflo and Harvey, 1985; Solanki, 1986; Sect. 3.2) also speaks against a purely stationary flow being the source of the Stokes V asymmetry.

The zero-crossing shift can be reduced if we use a turbulence velocity to produce part of the line broadening. Thus by broadening the 5250.2 Å line with a mixture of micro- and macroturbulence of amplitude $\sqrt{\xi_{mic}^2 + \xi_{mac}^2} \approx 1.5 - 2.0 \text{ km s}^{-1}$ we have been able to obtain a zero-crossing shift as small as $0.4 - 0.5 \text{ km s}^{-1}$, which is considerably closer to the upper bound of 0.25 km s^{-1} set by the observations. However, the additional turbulent velocity implies that we do not have a pure downflow.

Finally, if we accept that the temperature in the network is higher than in the plage regions considered here (as suggested by the analyses of Solanki and Stenflo, 1984; Solanki, 1986; Pantellini et al., 1987), we have a paradoxical situation. Due to increased line weakening the higher temperature leads to smaller asymmetries of the synthetic profiles in the network for a given velocity and magnetic field structure. The observed asymmetries, on the other hand, can be considerably larger than in the plage. Thus, we have been able to reproduce the observed network profile of 5250.2 Å with the network model of Solanki (1986) only by increasing both the velocity and the magnetic field gradients significantly.

5. Conclusions

In the present paper we have discussed the simplest mechanism proposed so far to produce the observed asymmetry of Stokes V, involving a stationary flow inside a magnetic element with a gradient along the line of sight. With the help of extensive numerical radiative transfer calculations we have investigated it in detail.

A comparison of the calculated profiles with the observations demonstrates the limitations of this mechanism. The following arguments summarize the case against a stationary flow as the sole responsible agent for the observed asymmetry.

—We are unable to reproduce the observed profiles (δA values) of e.g. Fe I 5250.2 Å and Fe I 5083.3 Å, or Fe I 5250.2 Å and Fe II 5197.6 Å simultaneously.

—We are unable to reproduce the asymmetry and the line-width of Fe I 5083.3 Å simultaneously.

—We are unable to reproduce the asymmetry and the zero-crossing shift simultaneously of any of the three lines: Fe I 5250.2 Å, Fe I 6301.5 Å, and Fe I 6302.5 Å.

We therefore conclude that *stationary* flows inside fluxtubes are *not* the main contributors to the asymmetry in the Stokes V profiles. This result is supported by the work of Ribes et al. (1985) who have calculated line profiles for the theoretical fluxtube models of Unno and Ribes (1979) which contain stationary downflows. The profiles they calculate also fail completely to match the observations.

Do these arguments imply that velocities are ruled out as the source of V asymmetry altogether? We believe not. Firstly, there is the indirect empirical evidence for a connection between asymmetry and velocity broadening presented by Solanki (1986). Secondly, large amplitude mass motions are present in fluxtubes which broaden the lines considerably, but do not significantly shift them. Due to the strong vertical stratification, gradients in velocity and magnetic field along the line of sight are bound to occur, while the presence of a current sheet at the boundary means that strong horizontal gradients in both the magnetic field and velocity are also present, even in small fluxtubes. Thus the velocity will automatically tend to produce some asymmetry in the line profiles. However, the non-stationary velocity structure will be considerably more involved than the simple $v(\tau)$ profiles considered here. For the purposes of empirical modelling it may be represented as the sum of many individual (stationary) $v(\tau)$, so that Stokes V profiles calculated for a large number of $v(\tau)$ will have to be summed up to give a resultant which can be compared to the observations. One problem with this approach is the large number of free parameters which makes a purely empirical analysis impractical. A physically self-consistent and dynamical model of fluxtubes is required (e.g. overstable oscillations model of Hasan, 1985; wave calculations as reviewed by Roberts, 1986, or Ulmschneider and Muchmore, 1986; dynamical solutions obtained with the code of Deinzer et al., 1984). This is beyond the scope of the present investigation.

We have also shown that velocity gradients should leave very weak lines with almost no area asymmetry. This can be used to distinguish between velocity-based and other possible mechanisms. However, observations with very high S/N ratio in a number of very weak lines are needed (more than one line is required in order to be certain that weak blends do not give a false signal).

We are well aware of the limitations of our approach. In particular the fact that only one dimensional models have been used in an attempt to fit data averaged over a number of magnetic elements. Thus it is possible that in reality velocities outside the magnetic elements also play a role in producing the asymmetry. We conclude that, although stationary flows inside the magnetic elements can, to our minds, be ruled out as the dominating source of Stokes V asymmetry, the broader question of whether velocity gradients in general are the main source of δA, or if the optical pumping mechanism of Kemp et al. (1984) plays the major role cannot be decided by this investigation. Both further observations and model calculations are required to settle this point conclusively.

References

Auer, L.H., Heasley, J.N.: 1978, *Astron. Astrophys.* **64**, 67
Beckers, J.M.: 1969, *Solar Phys.* **9**, 372

Chapman, G.A.: 1979, *Astrophys. J.* **232**, 923

Deinzer, W., Hensler, G., Schüssler, M., Weisshaar, E.: 1984, *Astron. Astrophys.* **139**, 426

Grigorjev, V.M., Katz, J.M.: 1975, *Solar Phys.* **42**, 21

Hasan, S.S.: 1985, *Astron. Astrophys.* **143**, 39

Illing, R.M.E., Landman, D.A., Mickey, D.L.: 1974a, *Astron. Astrophys.* **35**, 327

Illing, R.M.E., Landman, D.A., Mickey, D.L.: 1974b, *Astron. Astrophys.* **37**, 97

Illing, R.M.E., Landman, D.A., Mickey, D.L.: 1975, *Astron. Astrophys.* **41**, 183

Kemp, J.C., Macek, J.H., Nehring, F.W.: 1984, *Astrophys. J.* **278**, 863

Landi Degl'Innocenti E.: 1985, in *Theoretical Problems in High Resolution Solar Physics*, H.U. Schmidt, (ed.), Max Planck Inst. f. Astrophys., Munich, p. 162

Landi Degl'Innocenti, E., Landi Degl'Innocenti, M.: 1981, *Il Nuovo Cimento B* **62**, 1

Landi Degl'Innocenti, E., Landolfi, M.: 1983, *Solar Phys.* **87**, 221

Landman, D.A., Finn, G.D.: 1979, *Solar Phys.* **63**, 221

Makita, M.: 1981, in *Proc. Japan-France Seminar on Solar Physics*, F. Moriyama, J.C. Henoux, eds., University of Tokyo Press, Tokyo, p. 99

Makita, M.: 1986, *Solar Phys.* **106**, 269

Pahlke, K.D., Solanki, S.K.: 1986, *Mitt. Astron. Gesellschaft* **65**, 162

Pantellini, F.G.E., Solanki, S.K., Stenflo, J.O.: 1988, *Astron. Astrophys.* **189**, 263

Ribes, E., Rees, D.E., Fang, Ch.: 1985, *Astrophys. J.* **296**, 268

Roberts, B.: 1986, in *Small Scale Magnetic Flux Concentrations in the Solar Photosphere*, W. Deinzer, M. Knölker, H.H. Voigt, eds., Vandenhoeck and Ruprecht, Göttingen, p. 169

Scholiers, W., Wiehr, E.: 1985, *Solar Phys.* **99**, 349

Solanki, S.K.: 1985, in *Theoretical Problems in High Resolution Solar Physics*, H.U. Schmidt, ed., Max Planck Inst. f. Astrophys., Munich, p. 172

Solanki, S.K.: 1986, *Astron. Astrophys.* **168**, 311

Solanki, S.K.: 1987, *Ph.D. Thesis*, E.T.H. Zürich

Solanki, S.K., Keller, C., Stenflo, J.O.: 1987, *Astron. Astrophys.* **188**, 183

Solanki, S.K., Stenflo, J.O.: 1984, *Astron. Astrophys.* **140**, 185

Solanki, S.K., Stenflo, J.O.: 1985, *Astron. Astrophys.* **148**, 123

Stellmacher, G. Wiehr. E.: 1979, *Astron. Astrophys.* **75**, 263

Stenflo, J.O.: 1971, in *Solar Magnetic fields*, R. Howard (ed.), *IAU Symp.* **43**, 101

Stenflo, J.O., Harvey, J.W.: 1985, *Solar Phys.* **95**, 99

Stenflo, J.O., Harvey, J.W., Brault, J.W., Solanki, S.K.: 1984, *Astron. Astrophys.* **131**, 33

Stenflo, J.O., Solanki, S.K., Harvey, J.W.: 1987, *Astron. Astrophys.* **171**, 305

Stepanov, V.E.: 1958a, *Izv. Krymsk. Astrofiz. Obs.* **18**, 136

Stepanov, V.E.: 1958b, *Izv. Krymsk. Astrofiz. Obs.* **19**, 20

Ulmschneider, P., Muchmore, D.: 1986, in *Small Scale Magnetic Flux Concentrations in the Solar Photosphere*, W. Deinzer, M. Knölker, H.H. Voigt, eds., Vandenhoeck and Ruprecht, Göttingen, p. 191

Unno, W.: 1956, *Publ. Astron. Soc. Japan* **8**, 108

Unno, W., Ribes, E.: 1979, *Astron. Astrophys.* **73**, 314

Wiehr, E.: 1985, *Astron. Astrophys.* **149**, 217

Wittmann, A.D.: 1974, *Solar Phys.* **35**, 11